# An Oncolytic Adenovirus Targeting Transforming Growth Factor $\beta$ Inhibits Protumorigenic Signals and Produces Immune Activation: A Novel Approach to Enhance Anti-PD-1 and Anti-CTLA-4 Therapy

Yuefeng Yang,[1,2,†] Weidong Xu,[1,†] Di Peng,[3,†] Hao Wang,[2] Xiaoyan Zhang,[2] Hua Wang,[2] Fengjun Xiao,[2] Yitan Zhu,[4] Yuan Ji,[4] Kamalakar Gulukota,[5] Donald L. Helseth Jr.,[5] Kathy A. Mangold,[6] Megan Sullivan,[6] Karen Kaul,[6] Edward Wang,[7] Bellur S. Prabhakar,[8] Jinnan Li,[3] Xuejie Wu,[3] Lisheng Wang,[2] and Prem Seth[1,*]

[1]*Gene Therapy Program, Department of Medicine, NorthShore Research Institute, an Affiliate of the University of Chicago, Evanston, Illinois;* [2]*Department of Experimental Hematology, Beijing Institute of Radiation Medicine, Beijing, China;* [3]*Department of Urology, The Third Medical Center of Chinese People's Liberation Army, Beijing, China;* [4]*Program of Computational Genomics and Medicine,* [5]*Center for Personalized Medicine,* [6]*Department of Pathology and Laboratory Medicine, and* [7]*Biostatistics and Clinical Research Informatics, Department of Surgery; NorthShore University HealthSystem, Evanston, Illinois;* [8]*Department of Microbiology and Immunology, University of Illinois College of Medicine, Chicago, Illinois.*

[†]*These authors contributed equally to this work.*

In an effort to develop a new therapy for cancer and to improve antiprogrammed death inhibitor-1 (anti-PD-1) and anticytotoxic T lymphocyte-associated protein (anti-CTLA-4) responses, we have created a telomerase reverse transcriptase promoter-regulated oncolytic adenovirus rAd.sT containing a soluble transforming growth factor receptor II fused with human IgG Fc fragment (sTGF$\beta$RIIFc) gene. Infection of breast and renal tumor cells with rAd.sT produced sTGF$\beta$RIIFc protein with dose-dependent cytotoxicity. In immunocompetent mouse 4T1 breast tumor model, intratumoral delivery of rAd.sT inhibited both tumor growth and lung metastases. rAd.sT downregulated the expression of several transforming growth factor $\beta$ (TGF$\beta$) target genes involved in tumor growth and metastases, inhibited Th2 cytokine expression, and induced Th1 cytokines and chemokines, and granzyme B and perforin expression. rAd.sT treatment also increased the percentage of $CD8^+$ T lymphocytes, promoted the generation of $CD4^+$ T memory cells, reduced regulatory T lymphocytes (Tregs), and reduced bone marrow-derived suppressor cells. Importantly, rAd.sT treatment increased the percentage of $CD4^+$ T lymphocytes, and promoted differentiation and maturation of antigen-presenting dendritic cells in the spleen. In the immunocompetent mouse Renca renal tumor model, similar therapeutic effects and immune activation results were observed. In the 4T1 mammary tumor model, rAd.sT improved the inhibition of tumor growth and lung and liver metastases by anti-PD-1 and anti-CTLA-4 antibodies. Analysis of the human breast and kidney tumors showed that a significant number of tumor tissues expressed high levels of TGF$\beta$ and TGF$\beta$-inducible genes. Therefore, rAd.sT could be a potential enhancer of anti-PD-1 and anti-CTLA-4 therapy for treating breast and kidney cancers.

**Keywords:** TGF$\beta$, adenovirus, immunotherapy, breast cancer, kidney cancer

## INTRODUCTION

THE DEVELOPMENT OF NOVEL THERAPEUTICS for the treatment of metastatic breast, kidney, and other cancers is a major unmet need.[1,2] Transforming growth factor $\beta$ (TGF$\beta$) is a potent growth inhibitor under physiological conditions. However, during cancer progression, TGF$\beta$ can function as a protumorigenic factor.[3,4] In recent years, TGF$\beta$ signaling has emerged as a potential target for the treatment of advanced cancers.[5,6] Our laboratory has previously developed the oncolytic adenovirus Ad.sT, expressing soluble transforming growth factor receptor II fused with human IgG Fc fragment (sTGF$\beta$RIIFc).[7] sTGF$\beta$RIIFc can target TGF$\beta$ and therefore inhibit aberrant TGF$\beta$ signaling that is associated with many cancers.[7–9]

*Correspondence: Dr. Prem Seth, Gene Therapy Program, Department of Medicine, NorthShore Research Institute, Evanston, IL 60201. E-mail pseth@northshore.org



DOI: 10.1089/hum.2019.059

Direct inoculation of Ad.sT into established subcutaneous tumors in nude mouse inhibited tumor growth. In bone metastasis models of breast and prostate cancers in immunodeficient mice, systemic delivery of Ad.sT inhibited skeletal metastases.[8,10] However, the mechanisms of Ad.sT-mediated antitumor responses, particularly in immunocompetent mouse models, have not been examined.

In this study, we investigated the effect of intratumoral delivery of rAd.sT, an oncolytic adenovirus expressing sTGF$\beta$RIIFc, where E1 gene expression and the viral replication are regulated by human telomerase reverse transcriptase promoter (TERTp) in immunocompetent mouse tumor models of breast and renal cancers. Using a 4T1 mouse mammary tumor model in which the local tumors spontaneously metastasize to lungs and liver, we investigated rAd.sT-mediated inhibition of tumor growth and metastases. To understand the mechanisms of antitumor effects of rAd.sT, we examined the inhibition of TGF$\beta$ signaling pathways, and the systemic immune activation. We specifically examined TGF$\beta$1 expression, TGF$\beta$-inducible prometastatic factors, immunosuppressive Th2 cytokines, and antitumorigenic Th1 cytokines, granzymes, and perforin. In addition, we also investigated the activation of various immune cells in tumors, peripheral blood, and the spleen.

In recent years, immune checkpoint inhibitors, antibodies for antiprogrammed death inhibitor-1 (anti-PD-1) and anticytotoxic T lymphocyte-associated protein (anti-CTLA-4), have emerged as promising therapeutic agents for many cancers.[11–14] The clinical trials using anti-PD-1 have shown effectiveness against some triple negative human breast cancers.[2,11,14–16] However, many breast tumors are resistant to these treatments.[2,11,14–16] This resistance could be due to weak immunogenicity of the tumors, or poor inflammatory but highly immunosuppressive tumor microenvironment.[17–21] TGF$\beta$ is a strong immunosuppressor that can negatively affect the activity of anti-PD-1 and anti-CTLA-4.[22–26] To test this, we examined if rAd.sT, which expresses soluble TGF$\beta$RIIFc and targets TGF$\beta$, can improve the antitumor responses of anti-PD-1 and anti-CTLA-4 in a 4T1 tumor model. Finally, we investigated the expression of TGF$\beta$ as well as selected TGF$\beta$-inducible genes in the human breast and kidney cancer patients. Our findings show that rAd.sT could be developed for the treatment of breast and kidney cancers, and to improve the antitumor responses of anti-immune checkpoint inhibitors anti-PD-1 and anti-CTLA-4.

## MATERIALS AND METHODS

### Cell lines and adenoviruses

Human breast tumor cell lines, MCF-7 (ATCC, Manassas, VA) and MDA-MB-231 (kindly provided by Dr. Theresa Guise), were maintained as described earlier.[8] The mouse mammary tumor cell line, 4T1, and mouse renal tumor cell line, Renca, were purchased from ATCC. 4T1 cells were cultured in Eagle's minimal essential medium plus 10% fetal calf serum (FCS). Renca and human renal tumor cell lines, 786-O and 769-P (ATCC), were cultured in RPMI 1640 plus 10% FCS. Human embryonic kidney cells, HEK293 (ATCC), were cultured in Dulbecco's minimal essential medium supplemented with 10% FCS. All media components were purchased from Invitrogen (Grand Island, NY).

rAd.sT, a recombinant oncolytic adenovirus expressing sTGF$\beta$RIIFc, was constructed by using a simplified system[27] in which E1A expression is controlled by TERTp. rAd.Null, a control oncolytic adenovirus devoid of any foreign transgene, was also constructed. Nonreplicating adenoviruses, Ad(E1-).sT and Ad(E1-).Null, were constructed by the Ad-easy System as described earlier.[28]

### Adenoviral-mediated replication and cytotoxicity in tumor cells

Breast tumor cells (MDA-MB-231, MCF-7, and 4T1 cells) and renal tumor cells (786-O, 769-P, and Renca cells) were plated into a 6-well plate ($3\times10^5$ cells/well). The next day, cells were infected with $2.5\times10^4$ viral particles (VPs)/cell of adenoviruses. Three hours after infection, cells were washed with media, and crude viral lysates were either collected immediately or 48 h after infection. The viral titers in 3- or 48-h crude viral lysates were determined using the Adeno-X Rapid Titer Kit (Clutch, Mountain view, CA). Viral burst size (an increase in hexon-expressing positive cells from 3 to 48 h) was used as an indicator of viral replication as described earlier.[9]

To conduct cytotoxicity assays, breast and renal tumor cells were seeded into 96-well plates ($1\times10^3$ cells/well). The next day, cells were infected with various doses of adenoviruses (ranging from 2 to $1.25\times10^5$ VPs/cell) and continued to culture for 7 days. Cell survival was determined by sulforhodamine B staining, using uninfected cells as control as previously published.[29]

### Adenoviral-mediated sTGF$\beta$RIIFc expression in tumor cells

Breast and renal tumor cells were plated into 6-well plates ($3\times10^5$/well). The next day, cells were

infected with adenoviruses ($2.5\times10^4$ VPs/cell). Twenty-four hours after infection, cells were washed with phosphate-buffered saline (PBS), the media were changed to serum-free media, and the incubations continued for another 24 h. Cell lysates and media were collected separately. The sTGFβRIIFc protein in cell lysates and media was examined by Western blotting using antibody against human IgG, Fcγ fragment (Jackson ImmunoResearch, West Grove, PA), according to published procedures.[9] To quantify sTGFβRIIFc protein in media, enzyme-linked immunosorbent assay was conducted using the anti-human IgG, Fcγ fragment antibody and biotinylated anti-TGFβRII antibody (BAF241; R&D system, Minneapolis, MN), as described earlier.[9]

### Animal studies

All procedures for animal experiments were approved by the Institutional Animal Care and Use Committee (IACUC) at NorthShore University HealthSystem and at Beijing Institute of Radiation Medicine.

Evaluating rAd.sT efficacy *in vivo* in 4T1 and Renca tumor models in BALB/c syngeneic mice. To establish breast and renal tumor xenograft models, 4T1 or Renca cells were injected (day 0) into the right flank of 4–6-week-old BALB/c mice ($5\times10^6$ cells/mouse). On day 7 following tumor cell injections, tumor volumes were calculated by the following formula: tumor volume = width$^2\times$length/2. Tumor-bearing mice were divided into three groups, rAd.sT, rAd.Null, and buffer groups, without statistical differences among each group. On the same day (day 7), rAd.sT, rAd.Null ($2.5\times10^{10}$ VPs of each virus in 100 μL), or PBS was administered directly into the tumors. A second injection ($2.5\times10^{10}$ VPs of each virus or PBS) was administered on day 10.

In 4T1 model, tumor volumes were monitored on days 7, 10, 14, 18, 21, and 25. On day 12, four mice from each group were euthanized to conduct gene expression studies and histopathology. The remaining mice were euthanized on day 31. Tumors were harvested and the tumor weights were measured. sTGFβRIIFc gene and protein expression in the sera and tumor tissues were analyzed.

In the Renca tumor model, tumor growth was monitored on days 12, 15, 19, 22, 25, and 29. sTGFβRIIFc, TGFβ, and various TGFβ target gene expressions were examined on day 29.

For immune activation assays in the 4T1 model, four mice from each group were euthanized and peripheral blood cells, spleens, and tumor samples were evaluated on days 12, 18, and 31. In the Renca model, various immune assays were evaluated on days 12 and 29.

Immunophenotype analysis in the peripheral blood. On day 12, blood samples were collected and incubated with the following three different antibody panels for 30 min. Antibody panel 1: PerCP-Cy™5.5 rat anti-mouse CD45, APC hamster anti-mouse CD3e, FITC rat anti-mouse CD4 and PE rat anti-mouse CD8a. Antibody panel 2: FITC rat anti-mouse CD4, PE rat anti-mouse CD8a, PerCP-Cy™5.5 rat anti-mouse CD44 and APC rat anti-mouse CD62L. Antibody panel 3: FITC rat anti-mouse LY-6C and APC rat anti-mouse CD11b. The red blood cells were lysed by 1×RBC lysis solution according to the manufacturer's instructions (BD Bioscience, San Jose, CA). The immunophenotype of T lymphocytes, $CD4^+$ T memory cells, and myeloid-derived suppressor cells (MDSCs) was analyzed by flow cytometry. Various antibodies and other reagents for flow cytometry were purchased from BD Bioscience.

mRNA expression of various genes. Total RNA was isolated from tumor samples on day 12 and cDNA was synthesized using the RevertAid H Minus First Strand cDNA Synthesis Kit (Thermo Scientific, Wilmington, DE) according to the manufacturer's instructions. The mRNA expression of various genes listed in Supplementary Tables S1 and S2 was quantified by real-time reverse transcription PCR (real-time RT-PCR). The mRNA expression was quantified by Power SYBR Green PCR Master Mix on StepOnePlus real-time PCR system (Applied Biosystems/Life Technologies, Foster City, CA). The expression of the target genes was normalized by mouse β-actin expression.

Histopathological analysis and immunohistochemistry. On day 12, and at terminal time points, tumor tissues were harvested, processed, and stained with hematoxylin and eosin (H&E). Anti-human IgG, Fcγ fragment antibody was used to detect sTGFβRIIFc expression.

Immune evaluation in the spleen. On day 12 and at terminal time points, spleens were isolated, sliced into small pieces, and pressed through a 70-μm cell strainer (BD Falcon, Franklin Lakes, NJ). Single-cell suspensions were obtained and lysed by the RBC lysis buffer. The immunophenotypes of T lymphocytes were examined as described above for blood analysis. Single-cell suspensions were stained with Panel 1: FITC-conjugated anti-mouse CD4 antibody, PE-conjugated anti-mouse CD25

antibody, and APC-conjugated anti-mouse FoxP3 antibody; and Panel 2: FITC rat anti-mouse CD11c antibody (FITC-CD11c) and PE rat anti-mouse CD86 antibody (PE-CD86) (eBioscience, San Diego, CA). The percentage and number of antigen-presenting dendritic cells (DCs) in the spleen were analyzed by flow cytometry. The cytokine expressions in the spleen were detected by quantitative RT-PCR (qRT-PCR) as described above for the tumors.

### Zodiac analyses

Zodiac provides a comprehensive depiction of cancer functional interactions by integrating and analyzing multiomics cancer data from The Cancer Genome Atlas (TCGA).[30,31] It studies the interactions between multiple molecular entities of each pair of genes using novel Bayesian graphical models[32] through Markov chain Monte Carlo algorithms. Zodiac contains an interaction map for each of ~200 million genes and gene pairs. Statistical significance based on false discovery rate ≤0.1 leads to visualizing significant interactions between genomic entities. The data shown in this study (Supplementary Fig. S2) were directly obtained from the Zodiac website, which agrees well with our *in vitro* gene expression experimental data.

### Evaluating rAd.sT, anti-PD-1, anti-CTLA-4 combination therapy in 4T1 tumor metastasis model

4T1 cells were injected subcutaneously in female mice. On day 6, when the tumors were palpable, the tumor size was measured. On day 7, rAd.sT ($2.5 \times 10^{10}$ VPs in 50 $\mu$L) was administered directly into the tumors. A repeat viral dose was given on day 9. On days 8, 10, 12, and 14, anti-PD-1 and anti-CTLA-4 were administered intraperitoneally (each antibody dose used was 10 mg/kg of mouse weight). The tumor growth was monitored by caliper measurements. On day 25, mice were euthanized and lungs and liver were excised. Tumor lesions in the lungs and liver were counted. Tissues slices were subjected to H&E staining to confirm the metastatic lesions.

### Analyses of tumor tissues from human breast and renal cancer patients

Surgical specimens were obtained from 34 breast cancer patients and 19 renal cancer patients for clinical and pathological examination. All the samples were collected from 2010 to 2016 at the Beijing Friendship Hospital (Capital Medical University) and at the General Hospital of People's Armed Police Forces China. Based on the pathological examination, the surgical specimens were divided into tumor tissues, paracancerous tissues, and distal normal tissues. All the procedures were approved by the Ethics Committee of Beijing Friendship Hospital and General Hospital of People's Armed Police Forces China. The mRNA expression of TGF$\beta$ and its target genes listed in Supplementary Table S2 were detected by real-time RT-PCR.

### Statistical analyses

Data are presented as mean ± s.e.m. All statistical analyses were performed using GraphPad Prism software version 5 (GraphPad software, San Diego, CA). Longitudinal data were analyzed using a two-way repeated-measure analysis of variance (ANOVA) followed by Bonferroni *post hoc* tests for tumor growth data obtained over time. One-way ANOVA followed by Bonferroni *post hoc* tests were performed to analyze other data. Differences were considered significant at two-sided $p < 0.05$.

## RESULTS

### Characterization of rAd.sT *in vitro* and *in vivo*

rAd.sT produces sTGF$\beta$RIIFc protein, viral replication, and cytotoxicity in breast and kidney tumor cells in vitro. We first characterized rAd.sT in breast and renal cancer cells *in vitro*. Infection of the human and mouse breast and renal tumor cells with rAd.sT produced high levels of sTGF$\beta$RIIFc protein, which was also secreted into the extracellular media (Supplementary Fig. S1A, B). rAd.sT and rAd.Null infection produced high viral replication in the human tumor cells. However, only weak replication could be detected in the murine breast and renal tumor cells (Supplementary Fig. S1C). Interestingly, both rAd.sT and rAd.Null produced dose-dependent cytotoxicity in breast and renal tumor cells, including mouse cells (Supplementary Fig. S1D–E), suggesting that, in addition to viral replication, there might be additional mechanisms that contribute toward viral-induced cytotoxicity in the mouse cells.

Intratumoral inoculation of rAd.sT inhibits breast and renal tumor xenografts in immunocompetent mice. Next, we examined the rAd.sT-mediated antitumor responses *in vivo* in mouse tumor models. 4T1 mouse mammary tumors were established subcutaneously in immunocompetent BALB/c mice. rAd.sT and rAd.Null were administered directly into tumors, and the tumor growth was monitored over time. Results indicated that the

intratumoral injection of both rAd.sT and rAd.Null inhibited tumor growth. However, rAd.sT produced stronger inhibition ($p < 0.001$) (Fig. 1A). On day 25, mice were euthanized, and tumors were harvested and weighed. Compared with the buffer group, rAd.sT treatment significantly reduced tumor weight ($p < 0.01$) (Fig. 1B). Although the average metastatic area in the rAd.Null group is higher than that in the buffer group, there is no statistical difference between the buffer and rAd.-Null groups. In this experiment, the higher average data are attributed to larger individual differences in rAd.Null-treated mice.

Since 4T1 tumors are known to spontaneously metastasize to lungs, we also examined for lung metastasis on day 25. Significant lung metastasis was detected in the buffer-treated group. While rAd.Null did not inhibit the lung metastasis, a strong inhibition of lung metastasis was observed in rAd.sT-treated mice (Fig. 1C, D). rAd.sT-treated 4T1 tumors produced necrosis and expressed sTGF$\beta$RIIFc protein (Fig. 1E). High levels of sTGF$\beta$RIIFc were also secreted into the blood (Fig. 1F).

In the immunocompetent mouse Renca tumor model, rAd.sT and rAd.Null inhibited tumor growth; however, only rAd.sT produced significant inhibition of tumor weight (Fig. 1G, H). rAd.sT inoculation also produced high levels of sTGF$\beta$RIIFc protein in the tumors, and sTGF$\beta$RIIFc was also secreted into the blood (data not shown).

### Mechanistic studies: examination of tumor-promoting and metastasis-related genes, immunomodulatory factors, and immune cells

rAd.sT inhibits the expression of TGF$\beta$ target genes and alters the cytokine and chemokine expression in the tumors. We first investigated if the intratumoral delivery of rAd.sT can inhibit the expression of TGF$\beta$ and its target genes. Two days following vector delivery in the 4T1 tumors (referred to here as day 12), TGF$\beta$ and several angiogenesis- and metastasis-related genes (CTGF, PTHrP, CXCR-4, IL-11, VEGFA, VEGFR1, E-cadherin, N-cadherin, and vimentin) were analyzed by qRT-PCR in the tumor tissues. We have found that rAd.sT treatment downregulated the expression of these genes; however, the expression of E-cadherin was not altered (Fig. 2A). Reduced expression of selected genes that were examined (CTGF, PTHrP, and IL-11) was also observed in rAd.sT-treated Renca tumors (Fig. 2B). In these studies, rAd.sT generally produced stronger inhibition of TGF$\beta$ and TGF$\beta$ target genes compared with rAd.Null.

Since the intratumoral delivery of rAd.sT can induce tumor cell lyses, we postulated that it will augment antitumor responses due to the release of tumor-associated antigens. Therefore, we examined the expression profile of several cytokines and chemokines in tumor tissues on day 12 in 4T1 tumors. rAd.sT treatment reduced the expression of Th2 cytokines TGF$\beta$-1, IL-6, and IL-10 (Fig. 2C), while it increased the expression of Th1 cytokines TNF-$\alpha$, IL-2, IL-12, and IFN-$\gamma$ (Fig. 2C). Moreover, rAd.sT also increased granzyme B and perforin levels (Fig. 2C), the indicators of granule-mediated cytotoxicity. Taken together, these results suggest that rAd.sT treatment can activate various signals within the tumors that can potentially produce antitumor immune responses against the tumor tissues.

rAd.sT-regulated TGF$\beta$ target genes are also upregulated in human tumors in TCGA database. We have analyzed the connectivity of TGF$\beta$-1 with 11 TGF$\beta$ target genes, which were shown to be downregulated in rAd.sT-treated tumors as described above in Fig. 2. We used the Zodiac web query engine[31] to obtain the putative associations in Supplementary Fig. S2. Ten of 11 genes have positive transcriptional connectivity with TGF$\beta$-1, indicating a strong interaction of TGF$\beta$-1 with these genes in human cancer (there is no edge between gene expression (GE) of IL4* and GE of TGF$\beta$1) (Supplementary Fig. S2). Therefore, based on this analysis, it appears that the TGF$\beta$ regulatory pathways in 4T1 tumor model are quite similar to those observed in human cancers.

rAd.sT treatment increases $CD8^+$ T lymphocytes and $CD4^+$ T memory cells and reduces MDSCs in peripheral blood. In recent years, oncolytic viruses have attracted attention as vectors for immunogene therapy.[33–37] Cytotoxic T lymphocytes (CTLs) are the major immune effector cells that can kill tumor cells directly and produce antitumor responses. In the 4T1 xenograft model, the intratumoral delivery of rAd.Null and rAd.sT resulted in an increase of $CD8^+$ T cell percentage from $CD3^+$ T cells, while the percentage of $CD4^+$ cells was reduced. However, rAd.sT had much stronger effects on $CD8^+$ and $CD4^+$ T lymphocytes (Fig. 3A). Similar results were observed in the RENCA xenograft model (Fig. 3A). These results suggest that rAd.sT activated $CD8^+$ T lymphocytes, which can be induced to produce CTLs against the tumor cells. In future, it would be interesting to analyze if the memory T lymphocytes produced are indeed specific to 4T1 cells.

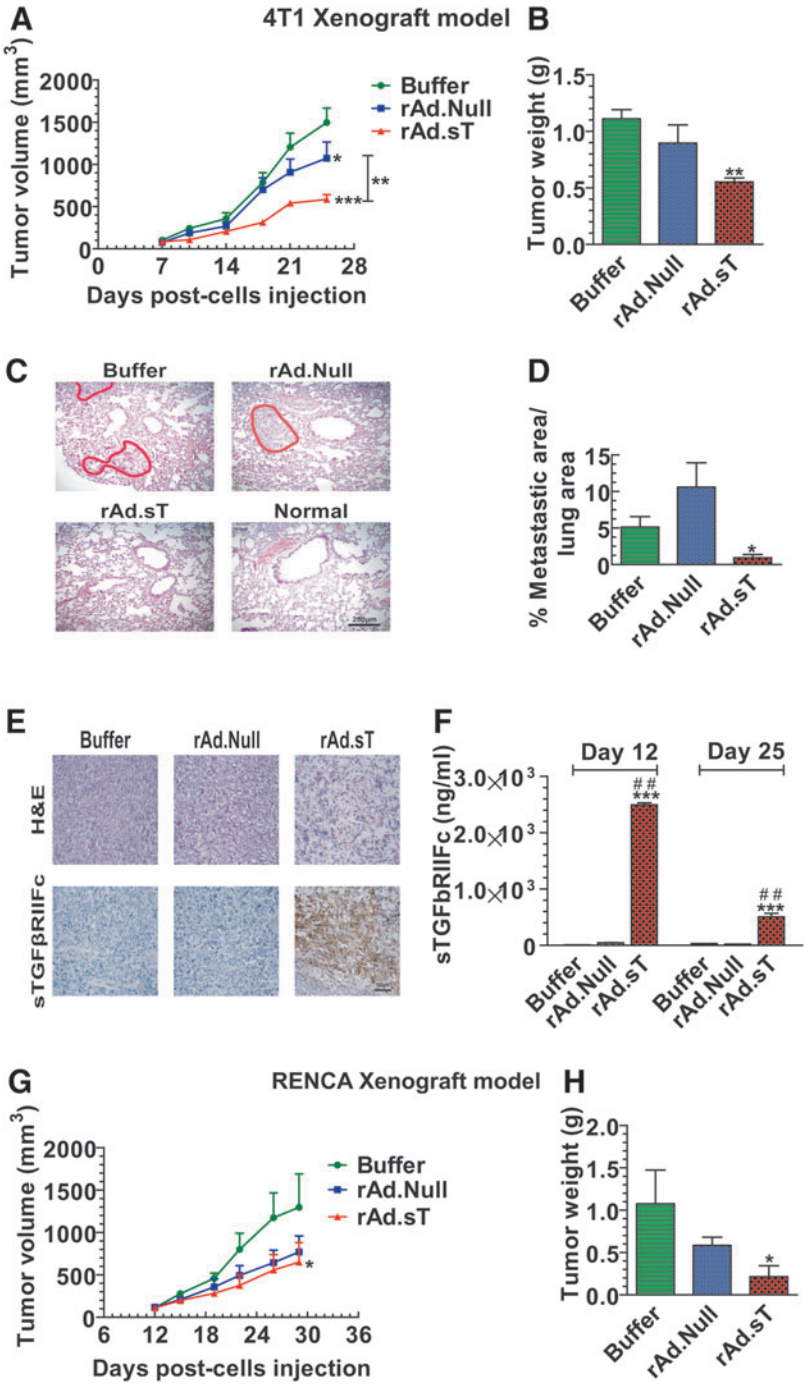


**Figure 1.** Intratumoral inoculation of rAd.sT inhibits tumor growth and metastasis in mouse 4T1 and Renca tumor xenograft models. 4T1 cells were injected subcutaneously into the right flank ($5\times10^6$ cells/mouse) of 4–6-week-old female BALB/c mice (day 0). On day 7, tumor-bearing mice were divided into three groups, buffer, rAd.Null, and rAd.sT groups ($n=10$/group). rAd.sT, rAd.Null ($2.5\times10^{10}$ VPs/100 $\mu$L), or PBS was injected intratumorally. On day 10, a repeat injection was administered. On days 7, 10, 14, 18, 21, and 25, the tumor sizes were measured **(A)**. On day 25, six mice from each group were euthanized, and the lungs and tumors were removed. Tumor weight was measured **(B)**. The tumor metastasis lesions in lungs were detected by H&E staining. The representative images are shown in **(C)**, and the metastatic areas in the lung were calculated **(D)**. The tumor tissues were stained with (H&E) and also subjected to immunohistochemistry for detecting sTGF$\beta$RIIFc expression **(E)**. On day 25, the sera were collected, and the sTGF$\beta$RIIFc protein was measured by ELISA **(F)**. Renca cells were injected under the right flank ($5\times10^6$ cells/mouse) of 4–6-week-old female BALB/c mice (day 0) to establish the subcutaneous renal model ($n=12$/group). Tumors were treated with oncolytic adenoviruses as described above. The tumor sizes were measured at days 12, 15, 19, 22, 25, and 29 **(G)**. On day 29, mice from each group were euthanized, and tumor weights were measured **(H)**. Data are shown as mean $\pm$ s.e.m. $^*p<0.05$; $^{**}p<0.01$; $^{***}p<0.001$ versus buffer group; $^{\#\#}p<0.01$ versus rAd.Null group. ELISA, enzyme-linked immunosorbent assay; H&E, hematoxylin and eosin; PBS, phosphate-buffered saline; sTGF$\beta$RIIFc, soluble transforming growth factor receptor II fused with human IgG Fc fragment; VP, viral particle.

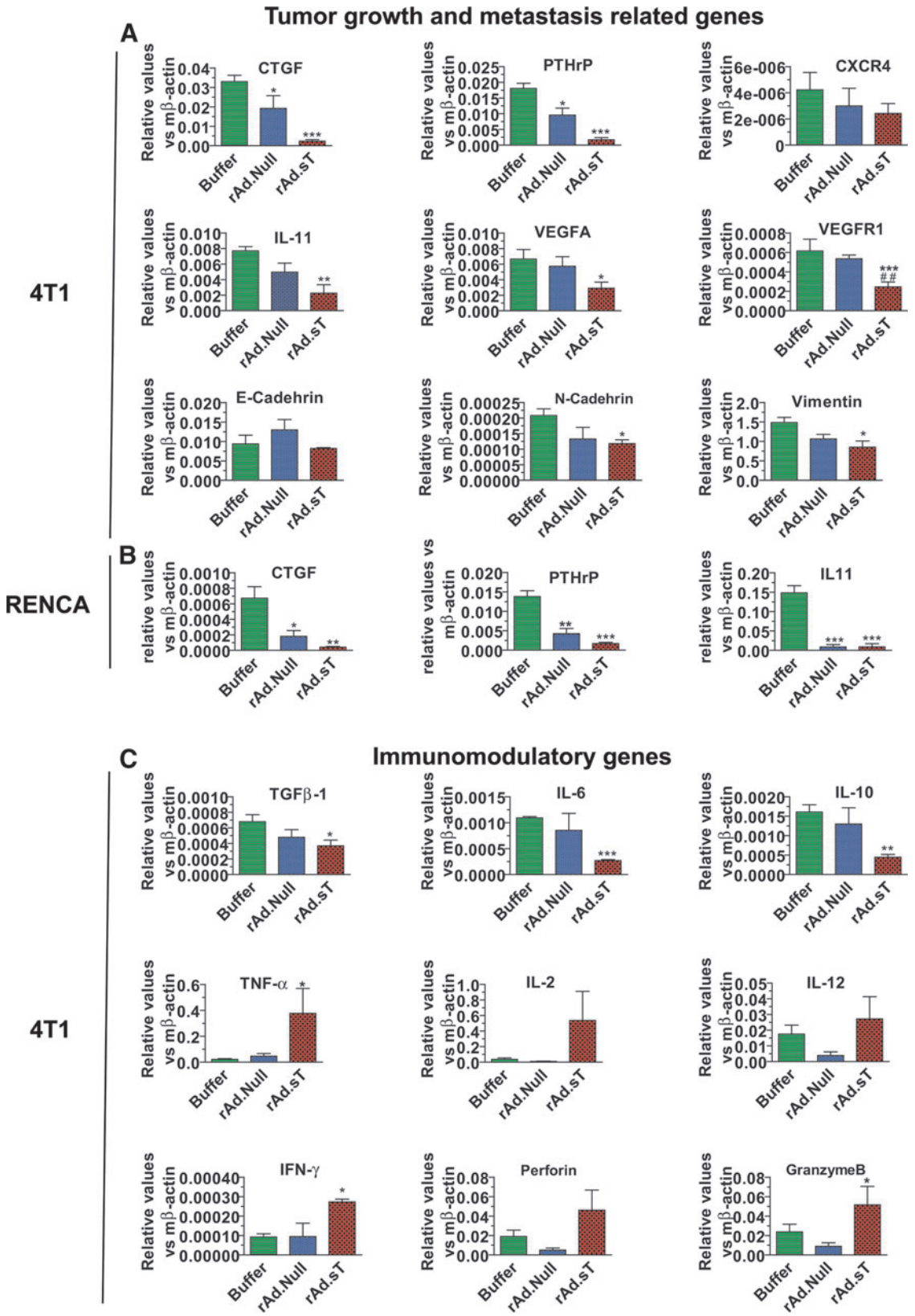


**Figure 2.** rAd.sT downregulates protumorigenic/metastasis, reduces Th2 cytokines, and increases Th1 cytokine and chemokine expression in the tumor microenvironment. On day 12 (2 days following adenoviral treatments), tumors in 4T1 and Renca xenografts were removed, and total RNA was isolated. After cDNA was synthesized, the expression of metastasis-related genes (CTGF, PTHrP, CXCR4, and IL-11), angiogenesis-associated genes (VEGFA and VEGFR), and epithelial/mesenchymal transition markers (E-cadherin, N-cadherin, and vimentin) was analyzed by real-time RT-PCR, and normalized by $\beta$-actin ($n=4$/group) **(A)**. In the murine Renca model, tumors were also collected 2 days following treatments with viruses. The expression of CTGF, PTHrP, and IL-11 was detected by real-time RT-PCR ($n=4$/group) **(B).** The expression of Th2 cytokines (TGF$\beta$1, IL-6, and IL-10), Th1 cytokines (TNF-$\alpha$, IL-2, IL-12, and IFN-$\gamma$), and chemokines (perforin and granzyme B) was detected by real-time RT-PCR in day 12 tumor tissues **(C).** ($n=4$/group). Data are presented as mean $\pm$ s.e.m. *$p<0.05$; **$p<0.01$; ***$p<0.001$ versus buffer group. RT-PCR, reverse transcription PCR.

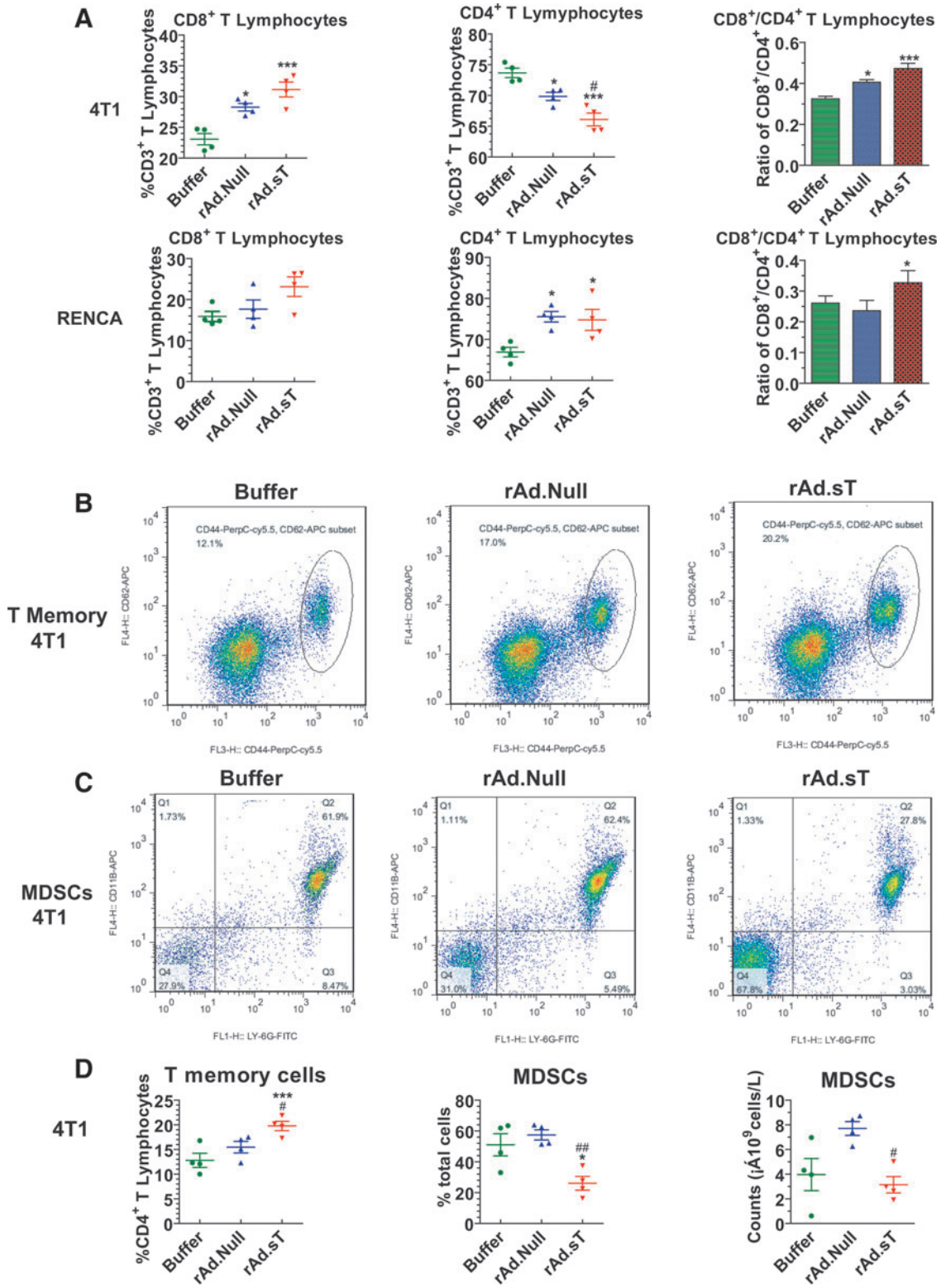


**Figure 3.** rAd.sT increases $CD8^+$ T lymphocytes and $CD4^+$ T memory cells, and downregulates MDSCs in the peripheral blood. On day 12, anticoagulant heparin-treated peripheral blood samples were collected from murine 4T1 and Renca tumor models. Blood cells were labeled with APC-conjugated anti-mouse CD3e, FITC-conjugated anti-mouse CD4, and PE-conjugated anti-mouse CD8 antibodies. The percentage of $CD8^+$ T lymphocytes and $CD4^+$ T lymphocytes was analyzed by flow cytometry **(A)**. Blood cells were also labeled with FITC-conjugated anti-mouse CD4, PerCP-Cy™5.5-conjugated anti-mouse CD44, and APC-conjugated anti-mouse CD62L antibodies. The percentage of T memory cells ($CD44^{High}CD62L^{High}$) among $CD4^+$ T lymphocytes was detected by flow cytometry. The representative images are shown **(B)**, and the statistical results are presented in **(D)**. Blood samples were labeled with FITC-conjugated anti-mouse Ly-6G and APC-conjugated anti-mouse CD11b, and analyzed by flow cytometry. The representative images are shown **(C)**, and the statistical analysis of the data is presented in **(D)**. Data are shown as mean ± s.e.m. $^*p<0.05$; $^{***}p<0.001$ versus buffer group; $^{\#}p<0.05$; $^{\#\#}p<0.01$ versus rAd.Null group. $n=4$ per group. MDSCs, myeloid-derived suppressor cells.

Interestingly, as shown above, rAd.sT has a completely opposite effect on $CD4^+$ T lymphocyte percentage in $CD3^+$ T lymphocytes in 4T1 and RENCA xenograft models, respectively (Fig. 3A). Although the results appear puzzling, following the delivery of oncolytic adenoviral vectors, as expected, $CD8^+$ T lymphocytes increased in the 4T1 as well as in the RENCA xenograft models. This is likely due to an anticipated antiviral response. In addition, our results suggested that Renca cells could promote a much stronger T cell proliferation than 4T1 cells and could also increase the number of T lymphocytes ($CD4^-CD8^-$T and $CD4^+CD\ 8^+$ T). Therefore, the $CD4^+$ cells in the buffer group of Renca model are lower. Furthermore, the different responses seen in 4T1 and RENCA xenograft models are likely due to different immunogenicity of these cells.

Next, we analyzed the generation of $CD44^{high}$ $CD62L^{high}$ T memory cells, which have recall responses against the tumors. We found that both rAd.Null and rAd.sT increased the percentage of $CD44^{high}CD62L^{high}$ T memory cells among $CD4^+$ T lymphocytes, however, rAd.sT treatment resulted in a significant increase ($p<0.05$) (Fig. 3B, D). Moreover, in rAd.sT-treated mice, the percentage of MDSCs and the total number of MDSCs in peripheral blood were significantly reduced (Fig. 3C, D). Therefore, we conclude that rAd.sT activated the $CD4^+$ T lymphocytes possibly via generating T memory cells, and downregulating the MDSCs in the peripheral blood. It is important to note that in the 4T1 xenograft model treated with rAd.sT, the $CD4^+$ T lymphocyte percentage in $CD3^+$ T lymphocytes was reduced, but the $CD44^{high}CD62L^{high}$ memory T lymphocyte percentage in $CD4^+$ T lymphocytes was increased. As one would expect, the CD4 T cell numbers go back to baseline levels on mounting an effective immune response; perhaps this return to baseline might explain the reduced CD4 T cell. Interestingly, $CD4^+$ T lymphocytes contain several subtypes, such as $CD44^{high}CD62L^{high}$ memory T lymphocyte, an important subtype required for the activation of antitumor immune recall responses. Here, we showed that rAd.sT could upregulate the percentage of $CD44^{high}CD62L^{high}$ memory T lymphocyte in $CD4^+$ T lymphocytes, suggesting an increase in the memory CD4 T cell pool. However, we could not determine if the increase of absolute number of $CD44^{high}CD62L^{high}$ memory T lymphocytes was statistically significant. We only conducted hemogram analysis from five mice in each group, and the corresponding samples were used for analyzing MDSCs. Therefore, we have not analyzed the absolute number of $CD44^{high}CD62L^{high}$ memory T lymphocytes.

In addition to $CD4^+$ central memory T lymphocytes, we did not analyze $CD4^+$ effector memory T lymphocytes and $CD8^+$ memory T lymphocytes for various memory phenotypes in this study. We will certainly pursue such detailed studies in our future efforts to clarify the immune activation mechanisms.

rAd.sT treatment upregulates $CD25^+FoxP3^+$Tregs and DCs in the spleen on day 18, while downregulates $CD25^+FoxP3^+$Tregs on day 31. The spleen is the site of production of several immune cells that play pivotal roles in immune activation. While we analyzed various immune cells present in the spleen, we also analyzed the immune suppressor $CD25^+FoxP3^+$Tregs cells in the 4T1 tumor model. On day 18, oncolytic viral treatments produced slight upregulation of regulatory T lymphocytes (Tregs), however, on day 31, significant reductions in the number and percentage of Tregs were observed (Fig. 4A, B). Interestingly, on day 31, the total number of spleen cells in the buffer group increased six to eight times ($7.07\times10^8$), compared with that on day 10 ($1.31\times10^8$). However, the Treg numbers increased disproportionately, suggesting selective expansion of Tregs, perhaps as a mechanism of immune evasion.

Another important observation is the reverse changes of Tregs in the spleen of 4T1 xenograft model on days 18 and 31. According to the results of hemogram analysis, the proliferation of T lymphocytes was induced following 4T1 cell incubation. Furthermore, we speculate that after adenoviral treatments, Tregs were initially induced to produce immune resistance to the viruses, which attributed to the upregulation of Tregs at early stage (day 18). However, at a later time point (day 31), rAd.sT delivery will produce high levels of target gene expression, thus blocking TGFβ activity and concomitant tumor cell lysis. Thus, at this time point, both the antitumor and antiviral immune responses are potentially activated, which could be associated with the reduction of Tregs.

The DCs play a central role in initiating, regulating, and maintaining antitumor responses. Therefore, we analyzed DCs in the spleen following adenoviral vector treatments. In the 4T1 tumor model, both rAd.Null and rAd.sT increased the total number and percentage of DCs in spleen on day 18 (Fig. 4C, D). However, on day 31, the elevated levels of DC percentages were sustained only in the rAd.sT-treated group (Fig. 4E). These results indicate that oncolytic adenovirus treatments could

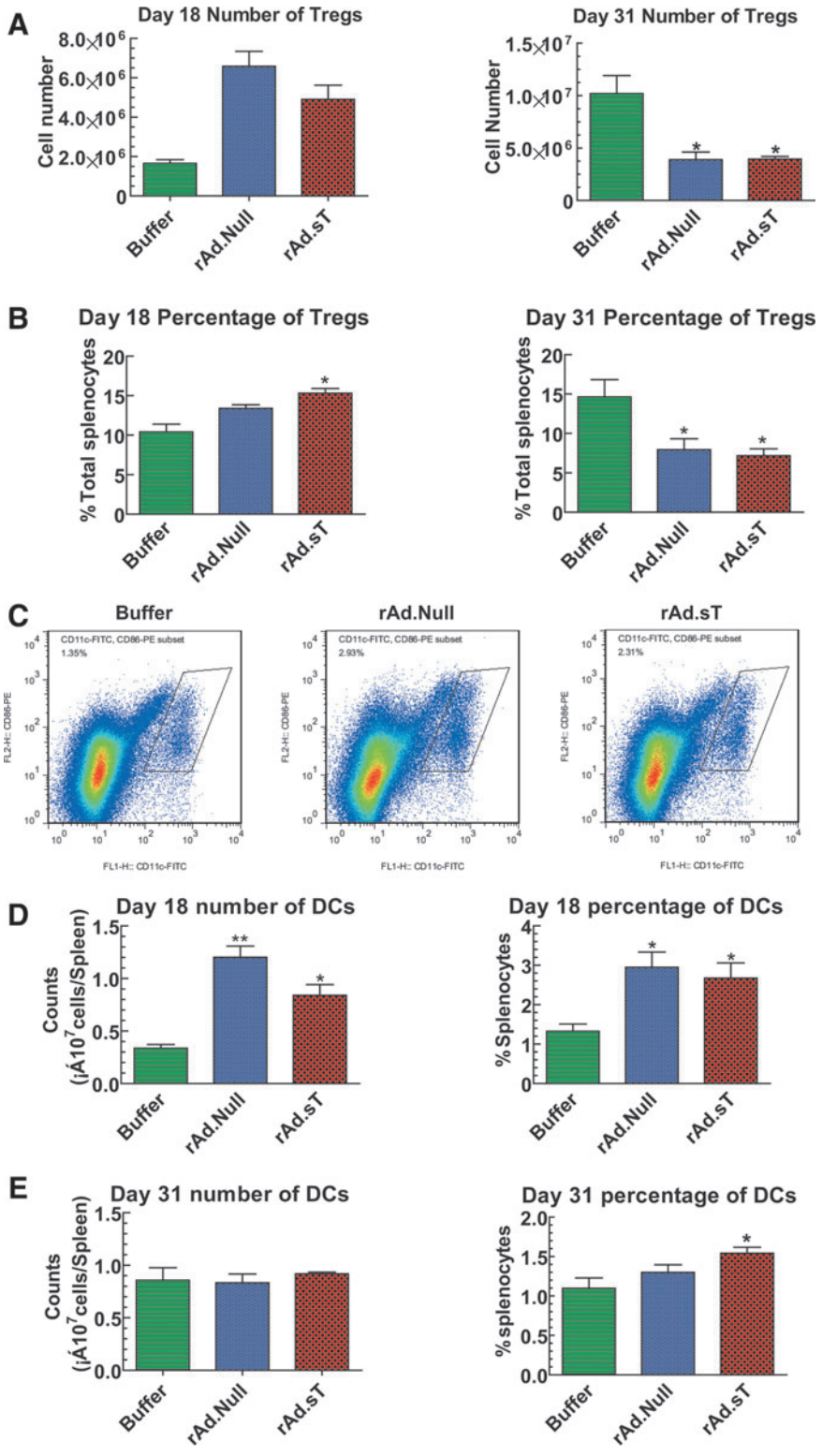


**Figure 4.** Effects of rAd.sT treatment on Tregs and DCs in the mouse spleen. Following various treatments, 4T1-bearing mice were euthanized at days 18 and 31. The spleens were removed and single-cell suspensions were prepared. After treating with RBC lysis buffer, splenocytes were counted. Then, cells were labeled with FITC-conjugated anti-mouse CD4 antibody, PE-conjugated anti-mouse CD25 antibody, and APC-conjugated anti-mouse FoxP3 antibody. The total number of $CD25^+FoxP3^+$ Tregs in spleen **(A)** and the percentage of Tregs in $CD4^+$ **(B)** were analyzed by flow cytometry. Moreover, cells were labeled with FITC-conjugated anti-mouse CD11c and PE-conjugated anti-mouse CD86 antibodies. The percentage of DCs ($CD11c^+CD86^+$) was examined by flow cytometry. The representative images on day 18 are shown in **(C)**. Quantification of DCs in days 18 and 31 samples is shown in **(D, E)**. Data are shown as mean ± s.e.m. $^*p<0.05$; $^{**}p<0.01$ versus buffer group. $n=4$ per group. DCs, dendritic cells; Tregs, regulatory T lymphocytes.

increase DCs, and rAd.sT could generate long-term responses.

In the 4T1 tumor model, oncolytic adenoviral treatment increased $CD4^+$ T lymphocytes on day 18, and as expected was slightly downregulated on day 31 (Supplementary Fig. S3A). Similarly, in the RENCA xenograft model, upregulation of $CD4^+$ T lymphocytes could also be detected in the spleen on day 12 (Supplementary Fig. S3B). We postulate that in peripheral blood, increase in $CD8^+$ T lymphocytes likely represented an antiadenovirus response, while in the spleen, $CD4^+$ T lymphocytes were activated likely due to antigen presentation by DCs in that organ where CD4T cells can in turn help $CD8^+$ T cells and other cells of the innate immune system. Our future detailed work should clarify this point.

Our *in vitro* experiments also showed that rAd.sT-infected 4T1 cells promoted spleen-derived T lymphocyte proliferation, induced Th1 cytokine expression (IL-2 and TNF-$\alpha$), and inhibited Th2 cytokine expression (IL-6 and IL-10). Some of these effects however, were also observed in rAd.Null-treated cells (Supplementary Fig. S4A–F).

### rAd.sT improves the antitumor effects of anti-PD-1 and anti-CTLA-4 in the 4T1 breast tumor model

We have observed significant rAd.sT-induced tumor necrosis in 4T1 tumors (Fig. 1E). This finding, along with the detection of high level of sTGF$\beta$RIIFc production that can potentially inhibit TGF$\beta$ pathways and thus alter the tumor microenvironment (as described above), suggests that the combination of rAd.sT and immune checkpoint inhibitors anti-PD-1 and anti-CTLA-4 can potentially be more effective in inhibiting tumor growth and metastases. To examine that, 4T1 tumors were established in BALB/c mice, and treatments with rAd.sT and anti-PD-1/anti-CTLA-4, either alone or in combination, were performed, as described in the Materials and Methods section. Tumor growth was followed over time till day 30. There was significant inhibition of tumor growth on treatment with either rAd.sT or anti-PD-1/anti-CTLA-4; however, the combination of rAd.sT and anti-PD-1/anti-CTLA-4 was more effective (Fig. 5A). On day 30, mice were euthanized and the lungs, liver, and spleen were collected, and the visible tumor lesions were counted. rAd.sT as well as anti-PD1/anti-CTLA-4 produced inhibition of lung metastases, however, the combination of rAd.sT and anti-PD-1/anti-CTLA-4 was the most effective approach (Fig. 5B). We have conducted histological examination of lung metastases. Large metastatic tumor lesions were clearly visible in the buffer-treated group. The tumors in the anti-PD-1/anti-CTLA-4 combination therapeutic group were smaller, but the smallest lesions were observed in the rAd.sT and anti-PD-1/anti-CTLA-4 combination group (Fig. 5C). These results indicate that, in the 4T1 tumor model, intratumoral inoculation of rAd.sT can improve the antitumor responses of anti-PD-1/anti-CTLA-4.

### Breast and renal cancer patients express high levels of TGF$\beta$ and TGF$\beta$ target genes in the tumors

To examine if human breast and kidney tumors express increased levels of TGF$\beta$ and TGF$\beta$ target genes compared to the distal normal tissues, we analyzed TGF$\beta$, CXCR4, PTHrP, and CTGF gene expression in human breast ($n=34$) and kidney tumor ($n=16$) tissues, and in the distal normal tissues. Increased expression of TGF$\beta$-1 was detected in 19 breast cancer patients (19/34) and 11 renal cancer patients (11/16) (Fig. 6A). In tumors expressing higher TGF$\beta$, metastasis-associated TGF$\beta$ target genes, CXCR4, PTHrP, and CTGF, were also upregulated in the majority of tumors (Fig. 6B, C). Please note that in breast cancer patients, we were able to analyze CTGF expression only in 14 tumor samples (Fig. 6B, D). Likewise, one sample from renal cancer patients was not enough to detect all of the genes. Therefore, only 10, but not 11, TGF$\beta$ upregulated samples were used to detect the expression of PTHrP, CXCR4, and CTGF (Fig. 6E).

Among the tumors with high TGF$\beta$-1 levels, significant upregulation of CXCR4 was detected both in the tumor tissues of breast and renal cancers. CXCR4 expression levels were increased in 17/19 and 8/10 samples of breast and renal cancer patients, respectively. However, a significant increase of CTGF expression was detected only in breast cancer (Fig. 6D–E). No significant upregulation of PTHrP was detected in either breast or kidney cancer patients. These results suggest that the increased TGF$\beta$ expression in breast and renal cancers could possibly promote tumor metastasis through upregulation of metastasis-related genes.

## DISCUSSION

In this study, we are reporting (1) the therapeutic effects of rAd.sT, an oncolytic adenovirus expressing soluble TGF$\beta$ receptor II Fc in 4T1 and Renca mouse tumor models, (2) the possible mechanisms of rAd.sT-mediated inhibition of tumor growth and metastases, (3) that rAd.sT can

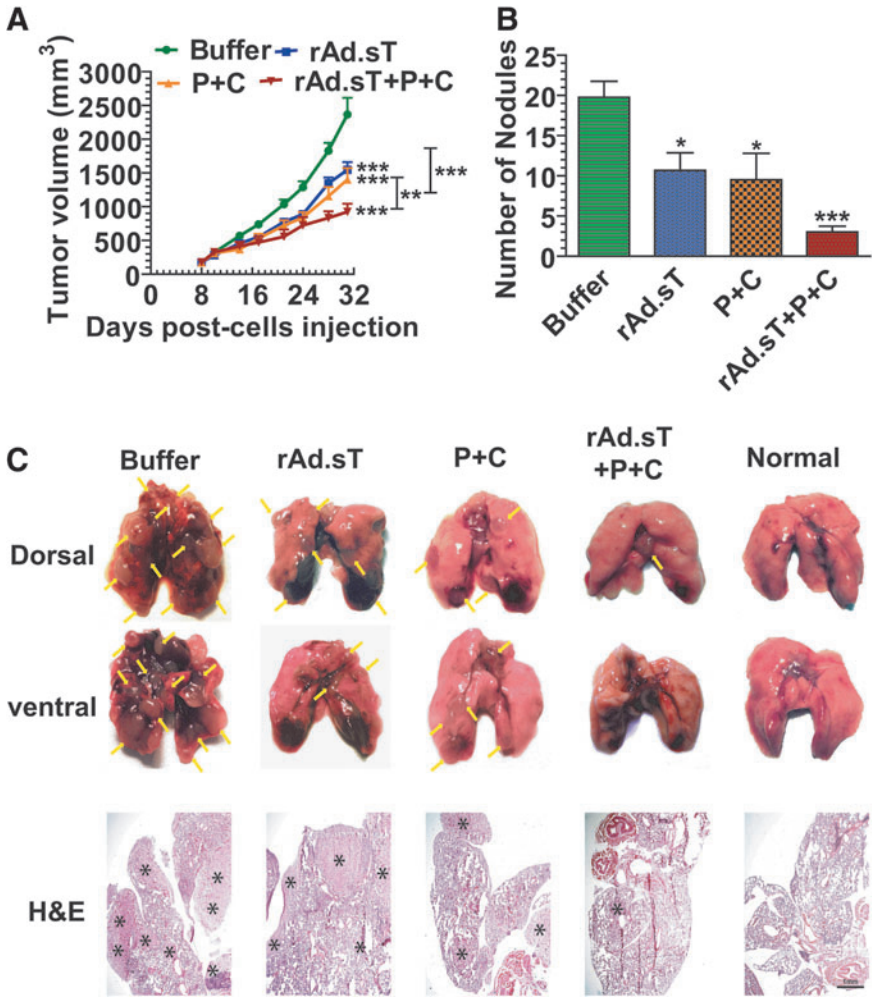


**Figure 5.** Combination therapy of rAd.sT with anti-PD-1 and anti-CTLA-4 antibodies in 4T1 xenograft. 4T1 cells were injected subcutaneously in female mice. On day 6, when the tumors were palpable, the tumor size was measured. On day 7, rAd.sT ($2.5\times10^{10}$ VPs in 50 $\mu$L) was administered directly into the tumors. A repeat viral dose was given on day 9. On days 8, 10, 12, and 14, anti-PD-1 and anti-CTLA-4 antibodies were administered intraperitoneally (10 mg/kg mouse weight). The tumor growth was monitored **(A)**, and mice were euthanized on day 30. The lungs were excised. Tumor lesions in the lungs were counted **(B)**, and the representative images are shown **(C)**. Tissues slices were subjected to H&E staining to confirm the metastatic lesions **(C)**. Data are shown as mean $\pm$ s.e.m. $^{**}p<0.01$, $^{***}p<0.001$ versus corresponding groups in **(A)**; $^{*}p<0.05$; $^{***}p<0.001$ versus buffer group in **(B)**. $n=8$ per group. anti-CTLA-4, anticytotoxic T lymphocyte-associated protein; anti-PD-1, antiprogrammed death inhibitor-1.

enhance the antitumor responses of anti-PD-1 and anti-CTLA-4 antibody in the 4T1 tumor model, and (4) significant numbers of breast and kidney patients' tumors have increased TGF$\beta$ and TGF$\beta$ target gene expression.

Based on our results presented here, we believe that rAd.sT-mediated inhibition of tumor growth and metastasis involves multiple mechanisms. Inoculation of rAd.sT in the tumors will directly lead to tumor cell death, with simultaneous production of sTGF$\beta$RIIFc in the tumors, and sTGF$\beta$RIIFc will be subsequently released into the blood. The production of sTGF$\beta$RIIFc *in situ* as well as the systemic presence in the blood will function as a TGF$\beta$ decoy, and thus inactivate TGF$\beta$ and block TGF$\beta$ signaling. The inhibition of TGF$\beta$-regulated genes CTGF, CXCR4, IL-11, PTHrP, N-cadherin, and vimentin, as reported here, is expected to directly affect tumor growth and metastases, as these proteins are well-documented inducers/markers of tumor growth, epithelial/mesenchymal transition, and metastases.[38–43] rAd.sT-mediated downregulation of VEGFA and VEGFR can also inhibit angiogenesis, and thus can also directly affect tumor growth.[44]

Our results also suggest that the intratumoral administration of rAd.sT produces a strong immune activation directed toward the tumors. rAd.sT-mediated induction of antitumorigenic Th1 cytokines (IL-2, INF-$\gamma$, IL-12) and the reduction of protumorigenic Th2 cytokines (TGF$\beta$, IL-6, IL-10), described here, will potentially have a direct effect

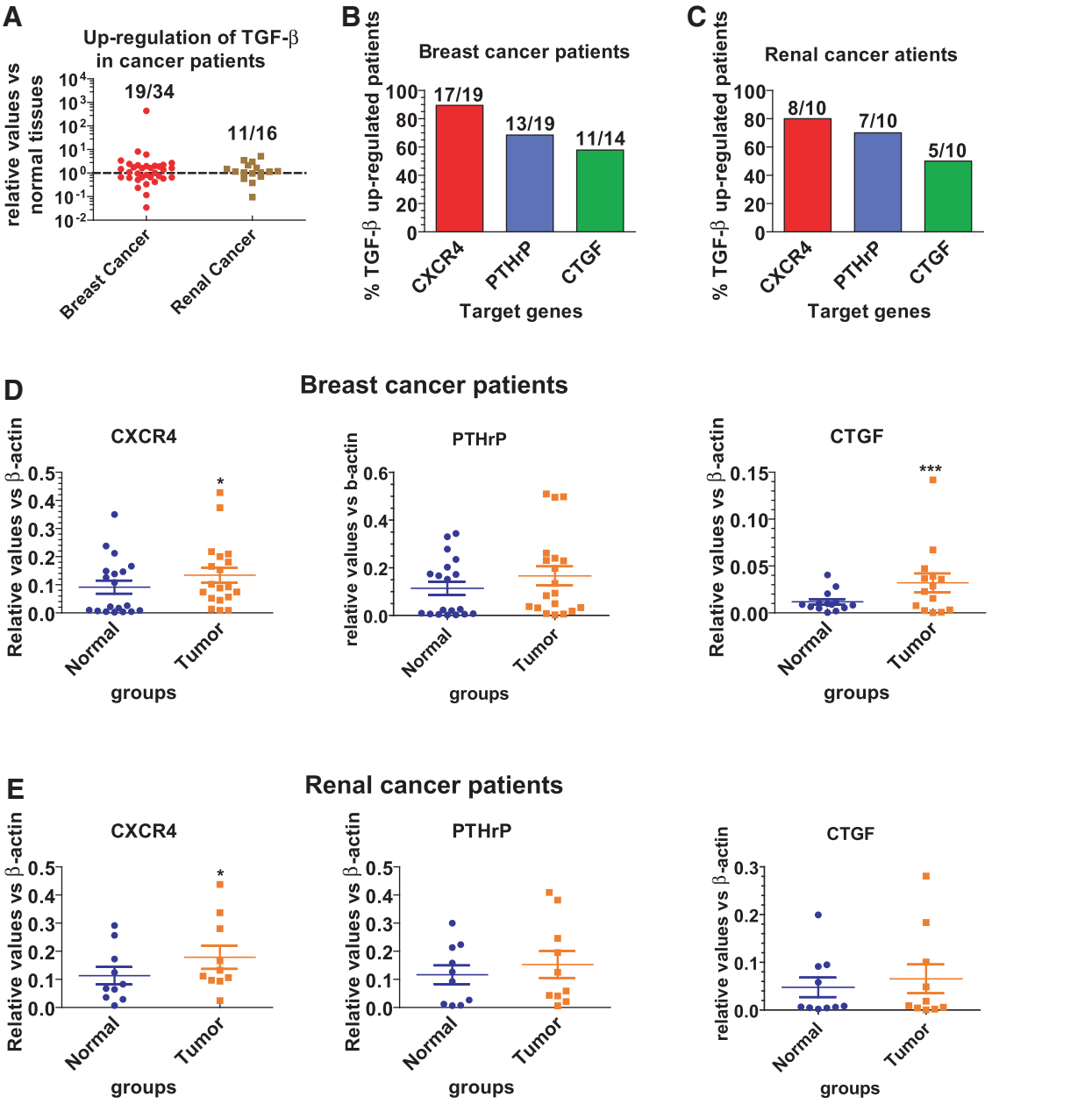


**Figure 6.** TGFβ and TGFβ regulatory genes are upregulated in breast and renal cancer patients. Surgical specimens were obtained from 34 breast cancer patients and 16 renal cancer patients for clinical and pathological examination. **(A)** TGFβ mRNA expression in the tumors. The TGFβ expression was measured by real-time RT-PCR in the tumor tissues and distal normal tissues. The relative expression of TGFβ in tumor tissues was normalized by that in normal tissues of the same patient. **(B–E)** Expression of TGFβ target genes in tumor tissues expressing higher TGFβ levels. The mRNA expression of CXCR4, PTHrP, and CTGF in breast cancer **(B, D)** and renal cancer patients **(C, E)** was detected by real-time RT-PCR. Data are shown as mean ± s.e.m. $*p<0.05$; $***p<0.001$ versus normal tissues. CTGF, connective tissue growth factor; PTHrP, parathyroid hormone-related protein; TGFβ, transforming growth factor β.

on the production and activation of T lymphocytes. In fact, rAd.sT treatment resulted in the upregulation of the $CD8^+$ T cells and $CD4^+$ T memory cells and enhanced the production and maturation of DCs. On the contrary, rAd.sT reduced the MDSCs and $CD4^+CD25^+$ Tregs. These results are consistent with other studies conducted in preclinical models, which showed that anti-TGFβ antibodies and small molecules targeting TGFβ signaling could restore the cytotoxicity of $CD8^+$ T lymphocytes, antigen presentation by DCs, and reduced $CD4^+CD25^+$ Tregs.[45–47] The induction of rAd.sT-mediated immunological cell death could also play a significant role in the antitumor responses, possibly by releasing damage-associated molecular patterns, further activating the immune cells via specific sensing pathways.[48,49] While many of the important steps and the cell types have been

identified in this proposed model, clearly studies into additional mechanisms, particularly the immune cell depletion experiments of $CD4^+$ T cells, $CD8^+$ T cells, Tregs, and MDSCs using appropriate antibodies, as well as the documentation of the rAd.sT-induced production of tumor-directed CTLs are further warranted.

An important point worth discussing is that a control replicating virus, rAd.Null, also produced some antitumor responses, although weaker than rAd.sT. This was particularly evident in the immune activation experiments, and was most obvious in the analyses of the immune cells in the spleen. This is not surprising as adenoviral-induced tumor cell death, as well as the immune activation directed against the virally infected cells, is not unexpected. While this antitumor effect could be beneficial, we realize that this could have some negative effects, for example, on the depletion of tumor-specific T cells. Therefore, one of the challenges in the future will be to identify strategies to minimize antiviral immune responses, while preserving and improving the tumor-specific immune responses.

The effect of rAd.sT-mediated enhancement of anti-PD-1 and anti-CTLA-4 therapy is of high significance. In recent years, there has been significant interest in developing anti-immune checkpoint inhibitors for cancer therapy. These inhibitors are already approved for several cancers, including melanoma and small-cell lung carcinoma.[11–14] In breast cancer, about one-third of triple-negative breast cancers also respond well to anti-PD-1. However, a large percentage of cancer patients are resistant to anti-PD-1/anti-CTLA-4 therapy.[11,14–16] Therefore, there is an interest in understanding the mechanism of anti-PD1-/anti-CTLA-4 resistance. One obvious reason for anti-PD1/anti-CTLA-4 resistance is the prevalence of the poor inflammatory environment in the tumors.[17–24,40,50,51] TGF$\beta$ plays a central role in inducing immune tolerance in the tumor microenvironment.[52,53] Furthermore, TGF$\beta$ has been shown to impair host immune responses to evade immune surveillance against the tumors.[25,26,54] We believe that rAd.sT-dependent immune activation as well as other nonimmune mechanisms described here could collectively contribute to the rAd.sT-mediated enhancement of anti-PD-1/anti-CTLA-4 therapy. In fact, recent studies have shown that the TGF$\beta$ can drive immune evasion in colon cancer metastasis,[25] and attenuate tumor response to PD-L1 blockade by contributing to the exclusion of T cells.[25,26] One advantage of using rAd.sT is that intratumoral inoculation of rAd.sT is expected to induce the host stimulator of interferon gene pathway of cytosolic DNA sensing, which can induce type I IFN production and DC activation, further augmenting anti-PD-1 therapy.[48,49,55] Regardless of the mechanisms, it is quite interesting that vectors such as rAd.sT can be easily applied in the clinical setting for cancer therapy as well as for improving anti-PD-1 and anti-CTLA-4 activity.

In this study, we have also shown that the tumors from human breast and kidney cancer patients express high levels of TGF$\beta$ and TGF$\beta$ target genes. Given the role of TGF$\beta$ in promoting tumor growth, invasion, and metastases, there is a significant interest in developing therapies targeted against TGF$\beta$. The patients expressing high levels of TGF$\beta$ and TGF$\beta$ target genes will be potential candidates for anti-TGF$\beta$ therapy. Several TGF$\beta$ inhibitors, including receptor kinase inhibitors antisense oligonucleotides and monoclonal antibodies, have been developed and investigated in preclinical animal models.[5,6] In fact, many clinical trials have also been conducted in cancer patients.[5,56] However, till today no anti-TGF$\beta$ inhibitor has been approved for cancer therapy. We have previously reported that systemic delivery of oncolytic adenovirus expressing sTGF$\beta$RIIFc can inhibit bone metastases in the mouse models of breast and prostate cancers.[8–10,28,57] It should be noted that the intratumoral delivery of oncolytic adenoviruses into multiple tumor types has been found to be safe and effective in several preclinical and clinical trials.[7,58–65]

In this study, we have used immunocompetent 4T1 and RENCA xenograft models. While human adenoviruses are able to kill 4T1 cells, in general, they replicate only weakly in mouse tumor cells. Therefore, these models do not exhibit the full therapeutic responses one might find in humans. Animal models such as NSG mice transplanted with human peripheral blood cells, which can support human tumor cell growth, could most likely produce much stronger antitumor responses and improvements of immune therapy. Before initiating clinical trials, we plan to use such models to conduct additional preclinical studies. Nevertheless, the studies described here, both direct inhibition of tumor growth and metastases, as well as the enhancement of anti-immune checkpoint therapy, can be potentially evaluated in the clinical setting and would find applications in the treatment of many cancers.

## ACKNOWLEDGMENTS

This work was funded, in part, by the National Institutes of Health Grants R01CA12738 (P.S.), a

pilot Clinical Translational Science Award (P.S.) from NorthShore University HealthSystem (NSUH), and a pilot breast cancer award (P.S.) from the Auxiliary of the NSUH. This work was also funded, in part, by the National Natural Science Foundation of China (No. 81402558 and 81472396) and the Nova Program of Beijing (Z171100001117118). The authors thank the Clinical Data and Biobank Resource of Beijing Friendship Hospital, Capital Medical University and General Hospital of People's Armed Police Forces for providing the human tumor samples. The funding agencies had no role in study design, data collection and analysis, and decision to publish or preparation of the manuscript. Prem Seth is thankful to Janardan Khandekar, Bruce Brockstein, Theodore Mazzone, Charles Brendler, and Michael Caplan for their continuous support.

## AUTHOR DISCLOSURE

No competing financial interests exist.

## SUPPLEMENTARY MATERIAL

Supplementary Figure S1
Supplementary Figure S2
Supplementary Figure S3
Supplementary Figure S4
Supplementary Table S1
Supplementary Table S2

## REFERENCES

1. Santa-Maria CA, Gradishar WJ. Changing treatment paradigms in metastatic breast cancer: lessons learned. JAMA Oncol 2015;1:528–534; quiz 549.
2. Nathan MR, Schmid P. The emerging world of breast cancer immunotherapy. Breast 2017; DOI: 10.1016/j.breast.2017.05.013.
3. Massague J. TGFbeta in cancer. Cell 2008;134: 215–230.
4. Katsuno Y, Lamouille S, Derynck R. TGF-beta signaling and epithelial-mesenchymal transition in cancer progression. Curr Opin Oncol 2013;25:76–84.
5. Akhurst RJ. Targeting TGF-beta signaling for therapeutic gain. Cold Spring Harb Perspect Biol 2017;9:pii: a022301.
6. Neuzillet C, Tijeras-Raballand A, Cohen R, *et al.* Targeting the TGFbeta pathway for cancer therapy. Pharmacol Ther 2015;147:22–31.
7. Seth P, Wang ZG, Pister A, *et al.* Development of oncolytic adenovirus armed with a fusion of soluble transforming growth factor-beta receptor II and human immunoglobulin Fc for breast cancer therapy. Hum Gene Ther 2006;17:1152–1160.
8. Hu Z, Zhang Z, Guise T, *et al.* Systemic delivery of an oncolytic adenovirus expressing soluble transforming growth factor-beta receptor II-Fc fusion protein can inhibit breast cancer bone metastasis in a mouse model. Hum Gene Ther 2010;21:1623–1629.
9. Hu Z, Gupta J, Zhang Z, *et al.* Systemic delivery of oncolytic adenoviruses targeting transforming growth factor-beta inhibits established bone metastasis in a prostate cancer mouse model. Hum Gene Ther 2012;23:871–882.
10. Hu Z, Gerseny H, Zhang Z, *et al.* Oncolytic adenovirus expressing soluble TGFbeta receptor II-Fc-mediated inhibition of established bone metastases: a safe and effective systemic therapeutic approach for breast cancer. Mol Ther 2011; 9:1609–1618.
11. Shin DS, Ribas A. The evolution of checkpoint blockade as a cancer therapy: what's here, what's next? Curr Opin Immunol 2015;33:23–35.
12. Hegde PS, Karanikas V, Evers S. The where, the when, and the how of immune monitoring for cancer immunotherapies in the era of checkpoint inhibition. Clin Cancer Res 2016;22:1865–1874.
13. Le DT, Durham JN, Smith KN, *et al.* Mismatch-repair deficiency predicts response of solid tumors to PD-1 blockade. Science 2017;357:409–413.
14. Vonderheide RH, Domchek SM, Clark AS. Immunotherapy for breast cancer: what are we missing? Clin Cancer Res 2017;23:2640–2646.
15. Pusztai L, Karn T, Safonov A, *et al.* New strategies in breast cancer: immunotherapy. Clin Cancer Res 2016;22:2105–2110.
16. Cimino-Mathews A, Foote JB, Emens LA. Immune targeting in breast cancer. Oncology (Williston Park) 2015;29:375–385.
17. Zamarin D, Postow MA. Immune checkpoint modulation: rational design of combination strategies. Pharmacol Ther 2015;150:23–32.
18. Hugo W, Shi H, Sun L, *et al.* Non-genomic and immune evolution of melanoma acquiring MAPKi resistance. Cell 2015;162:1271–1285.
19. Spranger S, Sivan A, Corrales L, *et al.* Tumor and host factors controlling antitumor immunity and efficacy of cancer immunotherapy. Adv Immunol 2016;130:75–93.
20. Gajewski TF, Fuertes M, Spaapen R, *et al.* Molecular profiling to identify relevant immune resistance mechanisms in the tumor microenvironment. Curr Opin Immunol 2011;23:286–292.
21. Shin DS, Zaretsky JM, Escuin-Ordinas H, *et al.* Primary resistance to PD-1 blockade mediated by JAK1/2 mutations. Cancer Discov 2017;7: 188–201.
22. Watanabe MA, Oda JM, Amarante MK, *et al.* Regulatory T cells and breast cancer: implications for immunopathogenesis. Cancer Metastasis Rev 2010;29:569–579.
23. Thomas DA, Massague J. TGF-beta directly targets cytotoxic T cell functions during tumor evasion of immune surveillance. Cancer Cell 2005;8:369–380.
24. Sheng J, Chen W, Zhu HJ. The immune suppressive function of transforming growth factor-beta (TGF-beta) in human diseases. Growth Factors 2015;33:92–101.
25. Tauriello DVF, Palomo-Ponce S, Stork D, *et al.* TGFbeta drives immune evasion in genetically reconstituted colon cancer metastasis. Nature 2018;554:538–543.
26. Mariathasan S, Turley SJ, Nickles D, *et al.* TGFbeta attenuates tumour response to PD-L1 blockade by contributing to exclusion of T cells. Nature 2018;554:544–548.
27. Hu ZB, Wu CT, Wang H, *et al.* A simplified system for generating oncolytic adenovirus vector carrying one or two transgenes. Cancer Gene Ther 2008;15:173–182.
28. Zhang Z, Hu Z, Gupta J, *et al.* Intravenous administration of adenoviruses targeting transforming growth factor beta signaling inhibits established bone metastases in 4T1 mouse mammary tumor model in an immunocompetent syngeneic host. Cancer Gene Ther 2012;19:630–636.
29. Katayose D, Gudas J, Nguyen H, *et al.* Cytotoxic effects of adenovirus-mediated wild-type p53 protein expression in normal and tumor mammary epithelial cells. Clin Cancer Res 1995;1:889–897.
30. Zhu Y, Qiu P, Ji Y. TCGA-assembler: open-source software for retrieving and processing TCGA data. Nat Methods 2014;11:599–600.

31. Zhu Y, Xu Y, Helseth DL, Jr., *et al.* Zodiac: a comprehensive depiction of genetic interactions in cancer by integrating TCGA data. J Natl Cancer Inst 2015;107;pii: djv129.

32. Mitra R, Müller P, Liang S, *et al.* A bayesian graphical model for ChIP-Seq data on histone modifications. J Am Stat Assoc 2013;108:68–80.

33. Rehman H, Silk AW, Kane MP, *et al.* Into the clinic: talimogene laherparepvec (T-VEC), a first-in-class intratumoral oncolytic viral therapy. J Immunother Cancer 2016;4:53.

34. Fountzilas C, Patel S, Mahalingam D. Review: oncolytic virotherapy, updates and future directions. Oncotarget 2017.

35. Lawler SE, Speranza MC, Cho CF, *et al.* Oncolytic viruses in cancer treatment: a review. JAMA Oncol 2017;3:841–849.

36. Russell SJ, Peng KW. Oncolytic virotherapy: a contest between apples and oranges. Mol Ther 2017;25:1107–1116.

37. Asad AS, Moreno Ayala MA, Gottardo MF, *et al.* Viral gene therapy for breast cancer: progress and challenges. Expert Opin Biol Ther 2017:1–15.

38. Guise TA, Mohammad KS, Clines G, *et al.* Basic mechanisms responsible for osteolytic and osteoblastic bone metastases. Clin Cancer Res 2006; 12:6213s–6216s.

39. Juarez P, Guise TA. TGF-beta in cancer and bone: implications for treatment of bone metastases. Bone 2011;48:23–29.

40. McAllister SS, Weinberg RA. The tumour-induced systemic environment as a critical regulator of cancer progression and metastasis. Nat Cell Biol 2014;16:717–727.

41. Valastyan S, Weinberg RA. Tumor metastasis: molecular insights and evolving paradigms. Cell 2011;147:275–292.

42. Kimbung S, Loman N, Hedenfalk I. Clinical and molecular complexity of breast cancer metastases. Semin Cancer Biol 2015;35:85–95.

43. Leblanc R, Peyruchaud O. Metastasis: new functional implications of platelets and megakaryocytes. Blood 2016;128:24–31.

44. Goel S, Wong AH, Jain RK. Vascular normalization as a therapeutic strategy for malignant and non-malignant disease. Cold Spring Harb Perspect Med 2012;2:a006486.

45. Tran TT, Uhl M, Ma JY, *et al.* Inhibiting TGF-beta signaling restores immune surveillance in the SMA-560 glioma model. Neuro Oncol 2007;9:259–270.

46. Tanaka H, Shinto O, Yashiro M, *et al.* Transforming growth factor beta signaling inhibitor, SB-431542, induces maturation of dendritic cells and enhances anti-tumor activity. Oncol Rep 2010;24: 1637–1643.

47. Liu VC, Wong LY, Jang T, *et al.* Tumor evasion of the immune system by converting CD4+CD25- T cells into CD4+CD25+ T regulatory cells: role of tumor-derived TGF-beta. J Immunol 2007;178:2883–2892.

48. Kroemer G, Galluzzi L, Kepp O, *et al.* Immunogenic cell death in cancer therapy. Annu Rev Immunol 2013;31:51–72.

49. Dudek AM, Garg AD, Krysko DV, *et al.* Inducers of immunogenic cancer cell death. Cytokine Growth Factor Rev 2013;24:319–333.

50. Sagiv-Barfi I, Kohrt HE, Czerwinski DK, *et al.* Therapeutic antitumor immunity by checkpoint blockade is enhanced by ibrutinib, an inhibitor of both BTK and ITK. Proc Natl Acad Sci U S A 2015; 112:E966–E972.

51. Li Y, Fang M, Zhang J, *et al.* Hydrogel dual delivered celecoxib and anti-PD-1 synergistically improve antitumor immunity. Oncoimmunology 2016;5:e1074374.

52. Teicher BA. Transforming growth factor-beta and the immune response to malignant disease. Clin Cancer Res 2007;13:6247–6251.

53. Yang L. TGFbeta and cancer metastasis: an inflammation link. Cancer Metastasis Rev 2010;29: 263–271.

54. Wojtowicz-Praga S. Reversal of tumor-induced immunosuppression by TGF-beta inhibitors. Invest New Drugs 2003;21:21–32.

55. Woo SR, Fuertes MB, Corrales L, *et al.* STING-dependent cytosolic DNA sensing mediates innate immune recognition of immunogenic tumors. Immunity 2014;41:830–842.

56. Herbertz S, Sawyer JS, Stauber AJ, *et al.* Clinical development of galunisertib (LY2157299 monohydrate), a small molecule inhibitor of transforming growth factor-beta signaling pathway. Drug Des Devel Ther 2015;9:4479–4499.

57. Xu W, Zhang Z, Yang Y, *et al.* Ad5/48 hexon oncolytic virus expressing sTGFbetaRIIFc produces reduced hepatic and systemic toxicities and inhibits prostate cancer bone metastases. Mol Ther 2014;22:1504–1517.

58. Barton KN, Stricker H, Elshaikh MA, *et al.* Feasibility of adenovirus-mediated hNIS gene transfer and 131I radioiodine therapy as a definitive treatment for localized prostate cancer. Mol Ther 2011;19:1353–1359.

59. Jiang H, Clise-Dwyer K, Ruisaard KE, *et al.* Delta-24-RGD oncolytic adenovirus elicits anti-glioma immunity in an immunocompetent mouse model. PLoS One 2014;9:e97407.

60. Larson C, Oronsky B, Scicinski J, *et al.* Going viral: a review of replication-selective oncolytic adenoviruses. Oncotarget 2015;6:19976–19989.

61. Li Z, Rakkar A, Katayose Y, *et al.* Efficacy of multiple administrations of a recombinant adenovirus expressing wild-type p53 in an immune-competent mouse tumor model. Gene Ther 1998;5:605–613.

62. Fujiwara T, Tanaka N, Kanazawa S, *et al.* Multicenter phase I study of repeated intratumoral delivery of adenoviral p53 in patients with advanced non-small-cell lung cancer. J Clin Oncol 2006;24:1689–1699.

63. Lambright ES, Force SD, Lanuti ME, *et al.* Efficacy of repeated adenoviral suicide gene therapy in a localized murine tumor model. Ann Thorac Surg 2000;70:1865–1870; discussion 1870–1861.

64. Freytag SO, Stricker H, Lu M, *et al.* Prospective randomized phase 2 trial of intensity modulated radiation therapy with or without oncolytic adenovirus-mediated cytotoxic gene therapy in intermediate-risk prostate cancer. Int J Radiat Oncol Biol Phys 2014; 89:268–276.

65. Jiang H, Fueyo J. Healing after death: antitumor immunity induced by oncolytic adenoviral therapy. Oncoimmunology 2014;3:e947872.

Received for publication March 30, 2019;
accepted after revision May 10, 2019.

Published online: May 24, 2019.